Journal of Optoelectronics and Advanced Materials, Vol. 4, No. 3, September 2002, p. 717 - 727

PHOTO-AND THERMALLY-INDUCED DIFFUSION AND DISSOLUTION OF Ag IN CHALCOGENIDE GLASSES THIN FILMS

T. Wagner

University of Pardubice, Department of General and Inorganic Chemistry,
Pardubice, 53210, Czech Republic

This paper is a review of our recent work that has been done to understand optically- and thermally-induced diffusion and dissolution (or solid state reaction) of silver in different chalcogenide glass films of As-S, As-Se and Ge-S systems. Kinetics of optically- and thermally-induced solid state reaction between silver and $As_{30}S_{70}$, $As_{30}Se_{70}$ and $Ge_{30}S_{70}$ films was measured by monitoring the change of thickness of the undoped chalcogenide using a modified computer-controlled reflectivity technique. Silver concentration profiles during optically-induced solid state reaction were traced by the means of Rutherford backscattering spectroscopy (RBS). The composition of the As-S, As-Se and Ge-S films was chosen to be $As_{30}S_{70}$, $As_{30}Se_{70}$, $Ge_{30}S_{70}$ which are compositions the most favorable for optically-induced solid state reaction, because they yield a homogeneous photodoped products. A new technique of step-by-step optically-induced dissolution and diffusion of Ag into $As_{30}S_{70}$, $As_{30}Se_{70}$, $Ge_{30}S_{70}$ amorphous films, which has allowed to design films with exact silver concentration and to study their properties has been applied. The host $As_{30}S_{70}$, $As_{30}Se_{70}$, $Ge_{30}S_{70}$ films were photodoped by consecutive dissolving of a thin (~10 nm) layers of silver, which resulted in homogeneous films of good optical quality. The silver concentration of the films ranged between 0 and 31 at.%. We have analysed the influence of the silver doping in the host material on optical and thermal properties, and its structure. The photodoped films produced were a single-phase homogeneous material. Results of all analytical techniques UV,VIS,NIR spectroscopy, temperature-modulated differential scanning calorimetry and Raman spectroscopy have helped to understand the processes taking place during silver photodissolution and its reaction products.

(Received July 12, 2002; accepted July 22, 2002)

Keywords: Chalcogenide glass, Silver dissolution, Thin film

1. Introduction

Optically- and thermally-induced diffusion and dissolution (OIDD) of metals such as Ag (Cu, Zn) into amorphous As-S, As-Se, Ge-Se and Ge-S chalcogenide semiconductors has been extensively studied by many researchers because of fundamental and technological interests [1-3]. Optically-induced dissolution of silver and diffusion into thin films of amorphous films with compositions $As_{30}S_{70}$, $As_{30}Se_{70}$, $Ge_{30}S_{70}$ have been in the focus of this review. It is also known that Ag-rich Ag-As-Se, Ag-As-S, Ag-Ge-S exhibit a phenomenon of so-called photo-induced surface deposition of metallic Ag, that is, photoinduced segregation of fine particles to the glass surface [4, 5]. Further it was found that these films exhibited reversibility in photo-writing and thermal-erasing of the Ag patterns [6]. The films of $Ag/As_{33}S_{67}$ and $Ag/Ge_{30}S_{70}$ has been recently shown as a useful material for fabrication of microrelief structures for preparation of phase diffractive optical elements [7, 8]. The glasses of Ag-Ge-S, Ag-As-S and Ag-As-Se systems belong also among so-called superionic conductors [9]. The interest this work was also to seek for new materials which are able to perform phase-change (crystalline to amorphous) optical recording (POR). Generally, such candidates are materials (e.g with stoichiometric compositions) which could be prepared in amorphous state and

crystalline state and using light-exposure of different energy to perform at best reversible transition. To consider the further development for application is essential to know the nature of the silver containing chalcogenide glass films, especially the optical, thermal and structural properties, since these physical properties are closely related to the mechanism of the POR phenomenon [10, 11]. Therefore, in our study we have prepared $Ag_x(As_{03}S_{0.7})_{100-x}$, $Ag_x(As_{03}Se_{0.7})_{100-x}$, $Ag_x(Ge_{03}S_{0.7})_{100-x}$ films by optically- induced step-by-step silver dissolution in $As_{30}S_{70}$, $As_{30}Se_{70}$, $Ge_{30}S_{70}$ evaporated films. Compositional dependence of the physical properties has been examined in a wide range of Ag contents by measurement of reaction kinetics; RBS, optical and Raman spectra; and thermal properties of the prepared films.

2. Experimental

The As-S, As-Se and Ge-S host films were prepared by using well-established vacuum evaporation technique. The bulk chalcogenide glasses used as an evaporation source were prepared from the constituent pure elements. Germanium, arsenic, selenium and sulphur of 5N purity were weighed and placed in precleaned and outgassed (by heating under vacuum to 900 ^oC) quartz ampoules. The ampoules were evacuated to a pressure of 1×10^{-3} Pa for 30 minutes and then sealed. The synthesis was performed in a rocking furnace with ampoules exposed to a temperature of 700 or 1050 ^oC for 24 hours. The fragments of the bulk material were evaporated from quartz crucible to avoid any contamination of the prepared layers. The layers were prepared on glass substrates in a 1×10^{-1} Pa vacuum, at a rate of 3-5 $nm.s^{-1}$. The obtained constant thickness layers were guaranteed by rotating substrate holders in planetary system. Thickness were monitored during evaporation with a quartz crystal monitor. The thickness of the $As_{30}S_{70}$, $As_{30}Se_{70}$ and $Ge_{30}S_{70}$ films were in the range of 800 to 1000 nm.

The silver concentration of the prepared samples ranged between 0 and 31 at.%. The composition of chalcogenide films (both doped and undoped) was analyzed by electron microprobe (using IXRF Systems).

Kinetics of optically-induced diffusion and dissolution of silver (d = 80 nm) in $As_{30}S_{70}$ and $Ge_{30}S_{70}$ (d = 800 nm) films was measured by monitoring the change in thickness of the undoped chalcogenide using a modified computer-controlled reflectivity technique [12]. The technique used to measure the rate of OIDD is based on the periodic variation of the reflectivity of a weakly absorbing film with its thickness, due to interference between light reflected from the top and bottom surfaces of the film. A typical plot of reflectivity as a function of exposure time during one of these experiments is shown in Fig. 1. The time between successive maxima or minima in the curve corresponds to the time required for the thickness of the undoped layer to decrease by $\lambda/2n$, or the doped layer to increase by $z\lambda/2n$, where λ is the wavelength of the detected light (λ = 550 nm), n is the refractive index of the undoped $As_{30}S_{70}$ and $Ge_{30}S_{70}$ layer at this wavelength (n = 2.3 and 1.9, respectively) and z is a constant relating the thickness of the doped layer to the thickness of the undoped material consumed (z = 1.07).

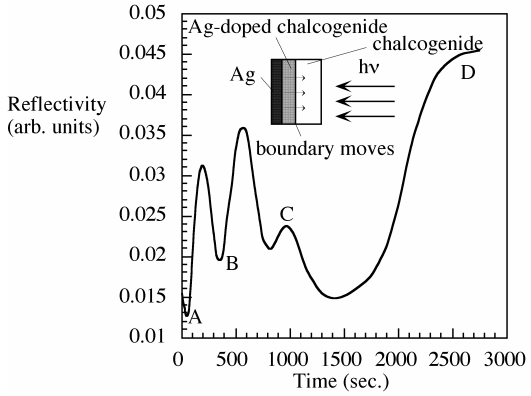

Fig. 1. A typical plot of optical reflectivity as a function of illumination time, for the $Ag/Ge_{30}S_{70}$ bilayer system during OIDD process.

Silver concentration profiles during OIDD were traced by the means of Rutherford backscattering spectroscopy (RBS) [13]. The RBS was chosen for the non-destructive measurement of the depth profile. We have measured RBS spectra of Ag/$As_{30}S_{70}$ and Ag/$Ge_{30}S_{70}$ (Fig. 2) samples using a 3490 keV alpha particles beam from accelerator at the Accelerator Laboratory of the Institute of Nuclear Physics in Rez. The RBS method is based on elastic scattering of mono-energetic ions which loose energy in scattering event is dependent on mass ration of projectile and scattering atom, and additional energy losses are caused by (weak) coulombic interaction with traversed matrix atoms. So mass and depth information is comprised in RBS spectra. The spectra were taken with the beam aligned at an incidence angle of 0^o with respect to the normal of the sample surface and with a backscattering angle of 170^o. The interactive computer program GISA 3.991 [14] was used for spectrum data evaluation. The overlapping of elemental signals in RBS spectra were partially separated due to the higher energy of alpha particles. The GISA code is able to extract depth profiles of Ag, Ge, S because for each depth at most only two of three signals shows overlapping. In reality, the concentration versus traversed amount of matter (in atoms/cm^2) can be determined. The conversion into depth profiles need some knowledge about density profiles. Some simple mathematical functions such as erf, normal, linear and constant profiles are included in GISA package. In spite of this difficulties, the RBS is practically the only method enabling (practically) non-destructive analysis of photochemical diffusion. The depth resolution rises from some 10 nm near surface due to the statistical "straggling" effect and the accessible depth is of some micrometers. The accuracy of method (in range of 2-5%) depends on knowledge of stopping powers, which enables to evaluate depth dependence due to the energy losses of projectile.

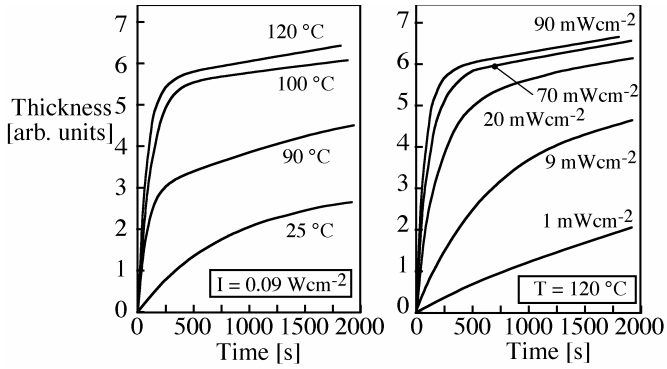

Fig. 2. Kinetics of OIDD process from the Ag layer into contact layer of $As_{30}S_{70}$ during heating. Curves are a parametric fits to experimental data (not shown in figure) using reaction kinetics model for differenr temperatures and exposure light intensity.

Further, we have analyzed in detail the influence of the silver doping in the host materials on optical and thermal properties, and its structure.

The thickness of the $As_{30}S_{70}$, $As_{30}Se_{70}$ and $Ge_{30}S_{70}$ films were in the range of 800 to 1000 nm, which are appropriate values for the accurate evaluation of optical parameters. Subsequently, constant thickness film (~10 nm) of silver was evaporated step-by-step on the top of the chalcogenide host. The host $As_{30}S_{70}$, $As_{30}Se_{70}$ and $Ge_{30}S_{70}$ films were photodoped by consecutive dissolving of thin (~10 nm) layers of silver, resulted in homogeneous films of very good optical quality. Photodoping was carried out by illuminating the samples by a lamp house equipped with large Fresnel lens, IR-cut filter and 250 W Tungsten lamp.

The optical transmission spectra of the films were recorded with Jasco V-570 UV/VIS/NIR spectrophotometer. According to Kosa et al. [15], the homogeneity of the doped thin-film samples was clearly confirmed by the corresponding spectral dependence of transmission, where no shrinkage of the interference fringes was observed. In order to calculate the thickness d, the refractive index n, and absorption coefficient α, from the thin film the transmission spectra, an evaluation method described by Swanepoel [16] was used. The maximum possible errors were evaluated as $\Delta n = \pm 0.005$ and $\Delta d = \pm 5$ nm.

The temperature-modulated differential scanning calorimetry (TMDSC, TA instruments 2920) technique has been applied to the measurement of the thermal properties of chalcogenide glasses of the silver doped $As_{30}S_{70}$, $As_{30}Se_{70}$ and $Ge_{30}S_{70}$ films. All samples in this work were exposed to the same temperature-modulated heating schedules with the average heating rate of 1 ^{o}C/min, temperature modulation amplitude ± 2 ^{o}C and period of 60 s. The total heat flow (HF), modulated heat flow (MHF), reversing heat flow (RHF) and a glass transition temperature T_g was determined. For the MDSC measurements the evaporated films and photodoped films were both mechanically peeled from the substrates, and immediately weighed into aluminium crimped pans and then properly sealed. A typical film sample weight was approximately 18 mg. The experimental errors of the T_g values are within a size of the data point symbol in the figure (see section 3).

Raman spectroscopy has been carried in the $As_{30}S_{70}$, $As_{30}Se_{70}$ and $Ge_{30}S_{70}$ films as silver was photo-doped into the host matrix. The Raman spectroscopy study was performed on a Fourier Transformation (FT) Raman spectrometer (Bruker, model IFS/FRA 106). Raman spectra were excited using a laser beam with λ = 1064 nm having an output power 50 mW. The wavelength of the laser beam was critical to avoid any photostructural change in these chalcogenide glasses within the time scale of 100 scans. The resolution of the Raman spectrometer was 1 cm^{-1}. The evaporated films and photodoped films were both mechanically peeled from the substrates, and immediately pressed into aluminium targets for the Raman measurements.

3. Results

3.1. Kinetics

The reflectivity oscillation curve (i.e., the position of the maxima and minima) in Fig. 1 was used to derive the experimental points for the kinetic curves in Fig. 2. In order to find the best physical model to describe and interpret our experimental data corresponding to the metal-dissolution kinetic measurements, four different fitting functions have been used.

It was found that the *measured* kinetic curve (i.e., doped layer thickness vs. exposure time), shown in Fig. 2, has a more complex character than was usually reported, and cannot be fitted by a simple square root function [17]. A much more realistic approach is to fit the experimental data using a composite function, as shown in Fig. 2, consisting of a single exponential and steady state terms, described previously in Ref. [18], two-stage exponential/linear model: $f(t) = -a\exp(-bt) + ct + d$, where b and c are the rate coefficients, and a and d are two constants. The parameters b and c are reaction rate coefficients ($a = k_{exp}$, $b = k_{lin}$ with units s^{-1}). The parameters a and d correspond to the photodoped layer thickness at the end of stage 1 and start of stage 2, respectively. The kinetics curve shows that there are two stages to the OIDD. The first stage is characterized by the rate coefficient k_{exp} and the second stage by k_{lin}, where $k_{exp} > k_{lin}$. The rate of OIDD, i.e. k_{exp} and k_{lin} in Ag/$As_{30}S_{70}$ and Ag/$Ge_{30}S_{70}$ systems increases with increasing temperature (293 to 393) and increasing light intensity (1 to 90 mW.cm^{-2}) as is clear from Table 1. Table 1 also shows activation energies of the two stages (E_{exp} and E_{lin}) as results of calculation from straight lines obtained from typical Arhenius plots (ln$k$ versus 1/T or lnk versus 1/I). Table 1 compares the results of kinetics obtained in Ag/$As_{30}S_{70}$ and Ag/$Ge_{30}S_{70}$ systems.

Table 1. The activation energies from Arhenius plots and parameter s obtained a results of parametric fits to experimental data of OIDD process for Ag/$As_{30}S_{70}$ and Ag/$Ge_{30}S_{70}$ systems.

Conditions	Sample	k_{exp} [s^{-1}] T=120 ^{o}C	k_{lin} [s^{-1}] T = 120 ^{o}C	$E_{a,exp}$ [kJ.mol^{-1}]	$E_{a,lin}$ [kJ.mol^{-1}]
k = f(T) I = 90 mWcm^{-2}	$As_{30}S_{70}$	3.4 10^{-2}	6.1 10^{-3}	22.5	33.3
	$Ge_{30}S_{70}$	1.2 10^{-2}	4.6 10^{-4}	20.5	40.2
k = f(I) T = 120 ^{o}C	$As_{30}S_{70}$	1.7 10^{-2} (I=70%)	3.0 10^{-3} (I=70%)	0.102	0.108
	$Ge_{30}S_{70}$	1.1 10^{-2} (I=70%)	1.0 10^{-3}(I=70%)	0.094	0.096

3.2. RBS spectra

The α particles RBS spectra shown in Fig. 3 (A), (B), (C), (D) were taken at different stages during the OIDD process in $Ag/Ge_{30}S_{70}$ system, i.e. for the unilluminated sample and for the illuminated samples with different illumination times in reference to Fig. 1. Similar results for $Ag/As_{30}S_{70}$ system could be find in [13]. The corresponding silver concentration depth profiles of the sample elements calculated from the α particles RBS spectra of the unilluminated and illuminated samples are shown in Fig. 4 (A), (B), (C) and (D), respectively. The results of the silver profile calculation yield information about the silver distribution in the samples after different illumination times and, as we believe, prove that the step-like profiles on the boundary of Ag-doped/undoped $As_{30}S_{70}$ and $Ge_{30}S_{70}$ films, are produced by illumination.

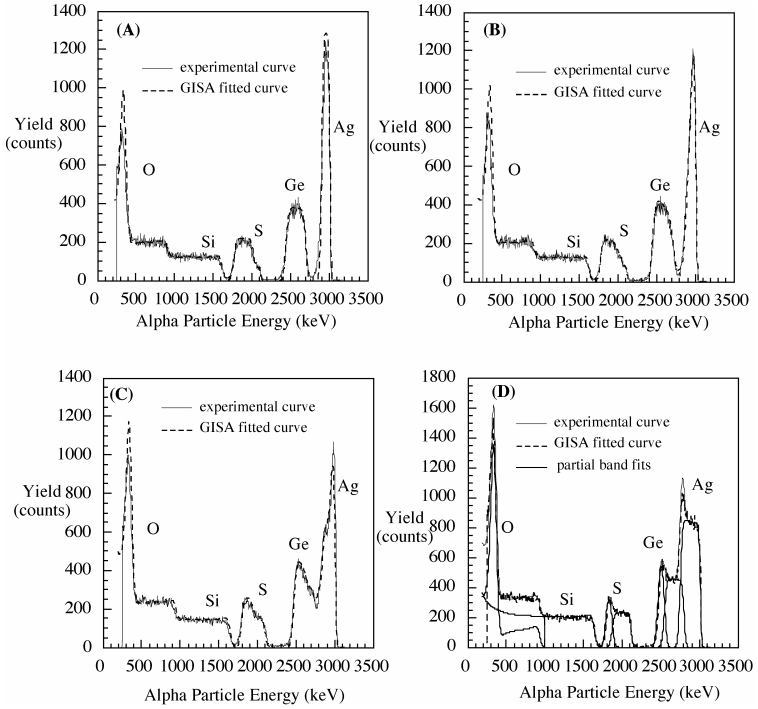

Fig. 3. A typical RBS spectra obtained in sample $Ag/Ge_{30}S_{70}$ sample after different illumination times are shown in (A) - (D) and corresponding to the reflectivity kinetic curve maxima and minima noted in Fig. 1.

3.3. Reaction product properties

To be able to study the properties of the different OIDD reaction products, we have prepared step by step OIDD Ag into $As_{30}S_{70}$, $As_{30}Se_{70}$ and $Ge_{30}S_{70}$ amorphous films, with silver concentration in a range from 0 to 31 at.%. The all films compositions have an accuracy of ± 0.5 at.%. The knowledge of composition of the evaporated films and films consequently synthesized by OIDD allowed to present dependences of optical thermal and structural properties on films compositions. It was proved that by using OIDD process, optically homogeneous films can be prepared with compositions which are not possible to produce by other methods, e.g. direct thermal evaporation or bulk glass synthesis because of restricted glass forming ability of Ag-As-S system [19]. This conclusion is valid also for prepared films and glass-forming ability in Ag-As-Se and Ag-Ge-S.

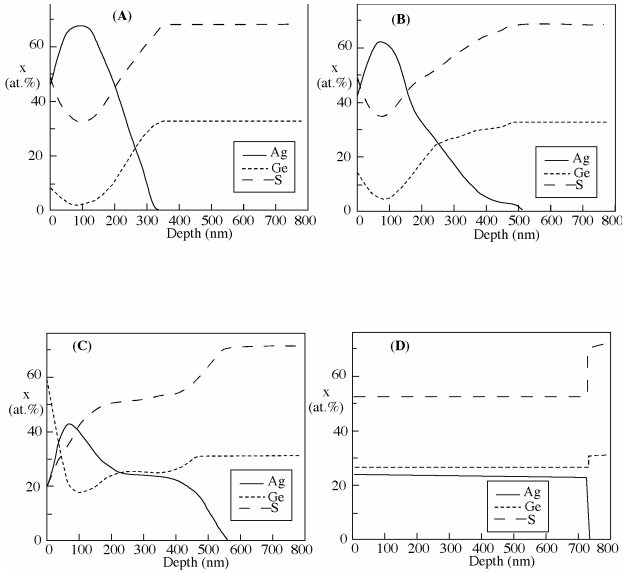

Fig. 4. The Ag, Ge and S concentration depth profiles (A) - (D), were obtained using GISA program from corresponding RBS spectra (A) - (D) in Fig. 3.

3.3.1. Optical constants

The typical optical transmission curves for films with composition $As_{30}S_{70}$ before and after OIDD of Ag and the calculated values the of spectral dependence of the refractive indexes *n*, in Fig. 5 demonstrate a significant shift of the optical egde and the increase in refractive indeces values for 24 at.% of built-in silver. The refractive index increase with increasing silver content for all studied films at constant wavelenght λ = 800 nm is presented in Fig. 6. As a consequence of optically silver dissolution and diffusion in $As_{30}S_{70}$, $As_{30}Se_{70}$ and $Ge_{30}S_{70}$ films, the significant decrease of $E_{g,opt}$, with increasing Ag content in the films, is shown in Fig. 7.

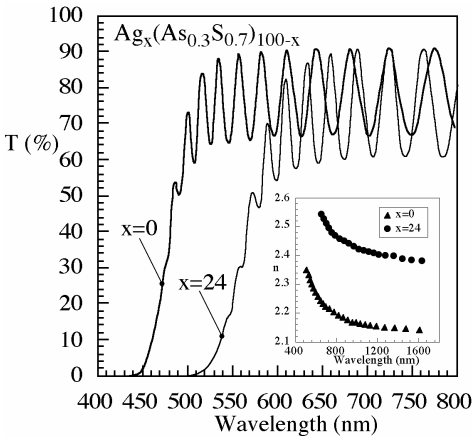

Fig. 5. Optical transmissivity and refractive index spectral dependence of $As_{30}S_{70}$ and silver optically -doped $As_{30}S_{70}$ films.

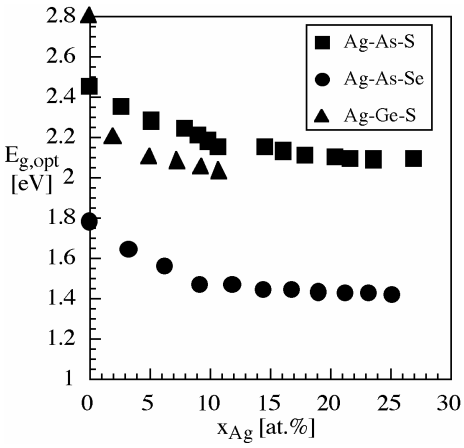

Fig. 6. Optical band gap, $E_{g,opt}$,vs. silver content dependence in prepared Ag-As-S, Ag-As-Se and Ag-Ge-S films.

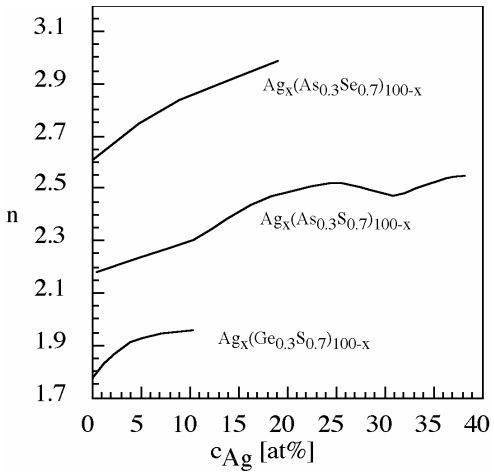

Fig. 7. Refractive index, n, vs. silver content dependence in Ag-As-S, Ag-As-Se and Ag-Ge-S films.

3.3.2. Thermal properties

Fig. 8 shows the dependence of the glass transition temperature T_g (taken at three important points of the sigmoidal C_p versus T curve [20], i.e. $T_{g,onset}$; $T_{g,inflex}$ and $T_{g,end}$), on composition of the Ag-As-S, Ag-As-Se and Ag-Ge-S films. The glass transition temperatures in all three sets of data and composition decreases with increasing Ag concentration down to a minimum between 5 and 10 at.%, then T_g increases.

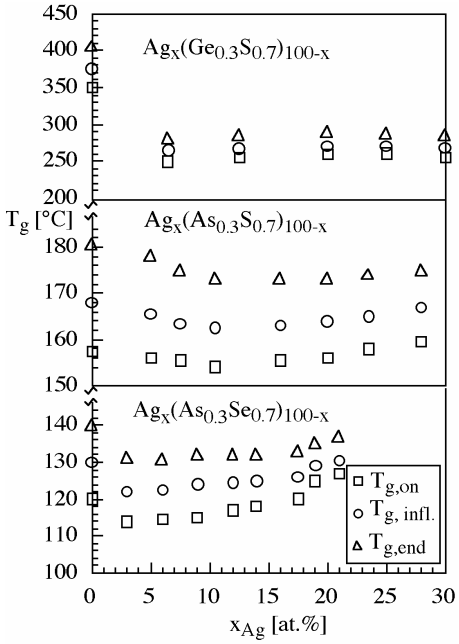

Fig. 8. Glass transition temperature vs. silver content dependence in Ag-As-S, Ag-As-Se and Ag-Ge-S films.

3.3.3. Raman spectroscopy

The Raman spectra measured in Ag-As-S, Ag-As-Se and Ag-Ge-S films are shown in Fig. 9, 10 and 11. The spectra of Ag-As-S films were interpreted using references [20-22]. The illuminated $As_{30}S_{70}$ film (Fig. 9, x = 0) contains strong bands at 333, 344 (units $AsS_{2/3}$) and 364 cm^{-1} (As_4S_4 units), and also weak bands at 474 and 496 cm^{-1} (S_8 rings or S rings fragments), respectively. The consequent step-by-step silver photodoping leads to an appearance of a new strong band at 376 cm^{-1} (AsS_3 pyramids connected by S-Ag-S linkage), and to a decrease of intensities of main bands and weak bands described for $As_{30}S_{70}$ film (Fig. 9, curves from x = 0 to x = 27 at.%).

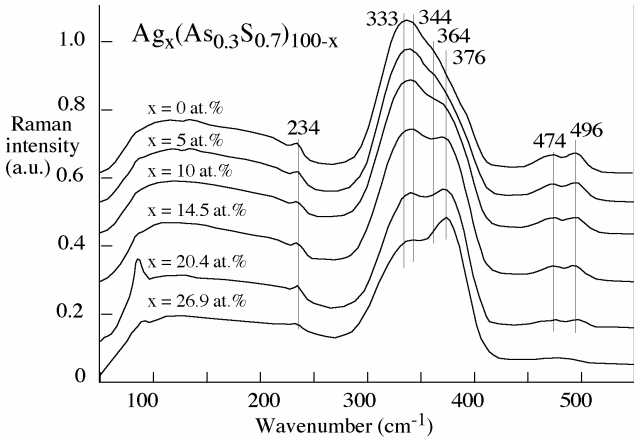

Fig. 9. Raman spectra of the prepared $As_{30}S_{70}$ and Ag-As-S films with given compositions.

The results of Raman spectroscopy studied in Ag-As-Se films are shown in Fig. 10. Spectra were interpreted using references [23-26]. The $As_{30}Se_{70}$ film (Fig. 10) contains strong bands at 227, 238, 256 and 270 cm^{-1}, multiple weak bands in spectral region 50-180 cm^{-1} and also weak band at 485 cm^{-1}, respectively. The silver step-by-step concentration increase leads to an appearance of a new strong bands at 248 and 205 cm^{-1}, also to an increase of the main band intensity 238 cm^{-1} then to an descrease of the 270 cm^{-1} band intensity, further to a shift of main band from 256 to 248 cm^{-1} and weak band shift from 485 to 465 cm^{-1}.

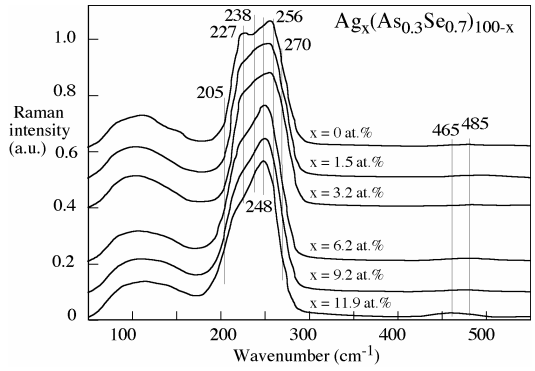

Fig 10. Raman spectra of the prepared $As_{30}Se_{70}$ and Ag-As-Se films with given compositions.

The Raman spectra measured in Ag-Ge-S films are shown in Fig. 11. The spectra were interpreted using references [27-30]. The $Ge_{30}S_{70}$ film (Fig. 11) contains strong bands at 343 (units $GeS_{4/2}$, corner sharing type ìCSî [29]), 374 cm^{-1} and 436 cm^{-1} ($GeS_{4/2}$ units, edge sharing type ìESî [29]), also weak band at 250 cm^{-1} ($GeS_{4/2}$ units, ethane-like type ìETHî [29]), and weak bands at 485, 218 and 155 cm^{-1} (S_8 rings or S rings fragments), respectively. The consequent step-by-step silver

photodoping leads to an increase of intensity of Raman band at 250 cm^{-1} (GeS_4, ETS units), and to a decrease of intensities of main bands 374 and 436 cm^{-1} ($GeS_{4/2}$, ES units), and disappearance of weak bands 485, 218 and 155 cm^{-1} assigned to S-S bonds presence (Fig. 11, curves from x = 0 to x = 31 at. %).

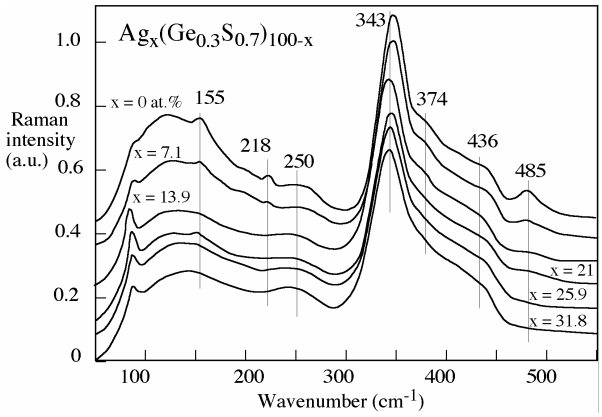

Fig. 11. Raman spectra of the $Ge_{30}S_{70}$ and Ag-Ge-S films with various compositions.

4. Discussion

The OIDD process consideration as a solid-state chemical reaction and proposed diffusion model are supported by *all* the *analytic* techniques used in the present work. The both kinetic data obtained are characterized by two rate coefficients, which implies that the OIDD process involves two different consecutive processes. It is suggested that in the *stage-1* (the exponential stage) a Ag-doped layer is formed. It is suggested that at the beginning of the exponential stage of OIDD, when the Ag-doped layer is formed and is *sufficiently* thin, the process can be influenced by electric space charges, resulting from the presence of a contact potential on the metal/p-type semiconductor boundary, which is the case for all studied Ag/chalcogenide bilayer system. These types of processes are frequently found during the formation of thin surface oxide layers on metals at low temperatures and are described by exponential or logarithmic rate law [31]. The *stage-2* (the linear stage) when the silver doped chalcogenide film is replacing undoped chalcogenide film in its volume, the overall reaction rate is driven by the reaction on the boundary Ag-doped/undoped chalcogenide, as described in [12]. The activation energies for stage 1 and stage 2 (E_{exp}, E_{lin}) are shown in Table 1 and their values are close to those characteristic of the diffusion process [18] in ion conductive glasses. It is also known from chemical kinetics theory that processes with activation energies E_a > 10 $kJ.mol^{-1}$ can be connected with chemical process. Ongoing chemical processes during OIDD were proved by Raman spectroscopy.

According to the results of the RBS measurements, the Ag concentration profile in the photodoped $Ge_{30}S_{70}$ and $As_{30}S_{70}$ [13] layer in the early stages of the OIDD process has a quite complicated character as can be seen in Fig. 4 (B). The Ag concentration profile is characterised initially by an exponential dependence on depth into the photodoped layer, but this changes during the OIDD process into a step-like dependence (Fig. 4 (C), as reported previously also for the $Ag/As_{33}S_{67}$ system [12]. All analytical technique used in this work show common and supporting results for the fact that it was possible by OIDD to prepare new Ag-As-S, Ag-As-Se and Ag-Ge-S materials with desired compositions in a range of silver concentration approximately from 1 to 31 at. %.

Optical transmissivity and optical parameters i.e. n and $E_{g,opt}$, show a strong evidence that silver is incorporated into and reacted with a host matrix of the $As_{30}S_{70}$, $As_{30}Se_{70}$ and $Ge_{30}S_{70}$ films. The decrease of $E_{g,opt}$, with Ag content increasing is clearly explained by the fact that the binding energies of Ag-S and As-As and Ge-Ge bonds are much smaller than those of the As-S, As-Se, Se-Se and S-S bonds [32] as shown in Table 2. Therefore, this leads to significantly smaller energy splitting between the states of the valence and conduction bands.

Table 2. Bond energies present in studied chalcogenide glasses [32].

Bond	As-S	As-Se	Ge-S	S-S	As-As	Ge-Ge	Se-Se	Ag-S	Ag-Se
Energy [kJ.mol^{-1}]	260	230	265	280	200	185	225	217	202

Measured thermal properties support the idea of optically-induced solid state reaction of silver in $As_{30}S_{70}$, $As_{30}Se_{70}$ and $Ge_{30}S_{70}$, as T_g is structurally sensitive parameter, which show a decrease of its value between 5 and 10 at. % Ag. The turning region around 10 at. % Ag can be phenomelogically described as a transition from the role of silver as glass modifier to glass former. The role of silver as a glass modifier or even the role of silver as a depolymerizer is evident from Raman spectra (Fig. 9, 10 and 11) in a built-in concentration range of 1-31 at. % Ag. Silver can create either one bond at the S-chain or Se-chain end or can break S-S or Se-Se bond in chains or rings. Their disapearance is clearly seen in Raman spectra (Fig. 9, 10 and 11). Optical transmission and Raman spectra of Ag-As-S films show also the homogenous reaction products up to x = 27 at. % Ag and similar results can be seen for other studied system Ag-As-Se and Ag-Ge-S. This fact proves that photoinduced reaction could lead to the same reaction products as a high temperature synthesis in a melt.

5. Conclusions

The kinetics and RBS spectra of the OIDD of Ag with $As_{30}S_{70}$, $As_{30}Se_{70}$ and $Ge_{30}S_{70}$ films were measured. The kinetics data show two stage reaction process (exponential and linear). RBS spectra show the step-like silver profile. It was also documented that using the OIDD process, the silver content can be reached in a broad concentration range in the final reaction products. The Ag-As-S, Ag-As-Se and Ag- Ge-S films were prepared as a single-phase homogeneous material in the concentration region 0 to 31 at.% Ag. Results of the analytical techniques have helped to understand the OIDD as silver dissolves in the host chalcogenide films and forms there Ag-S or Ag-Se bond which is documented by decrease of S-S or Se-Se bonds and by increase of structural units containing As-As and Ge-Ge bonds.

Acknowledgements

The author thanks grants 203/02/0087 and 203/00/0085 of the Grant Agency of Czech Republic, to Research Centre project LN00A028 of Ministry of Education, Youth and Sports Czech Republic and to University of Saskatchewan, Canada (prof. S. O. Kasap), for providing financial support for this project.

References

[1] A. V. Kolobov, Ka. Tanaka, Hand on Advanced Electronic and Photonic Materials, Academic Press, Tokyo 2000.
[2] Ke. Tanaka, H. Sanjoh, Defect and Diffusion Forum, **95-98**, 1213 (1993).
[3] T. Wagner, Assoc. Prof. Thesis, University of Pardubice, Pardubice, 2001.
[4] T. Kawaguchi, S. Maruno, J. Appl. Phys. **77,** 628 (1995).
[5] T. Kawaguchi, S. Maruno, S. R. Elliott, J. Appl. Phys. **79,** 9096 (1996).
[6] T. Kawaguchi, S. Maruno, Jpn. J. Appl. Phys. **33,** 6470 (1994).
[7] J. Eneva, A. Gushterov, B. Tomerova, B. Mednikarov, J. Mat. Sci.: Materials in Electronics **10,** 529 (1999).
[8] T. Wagner, G. Dale, P. J. S. Ewen, A. E. Owen, V. Perina, J. Appl. Phys. **87,** 7758 (2000).
[9] E. Robinel, B. Carette, M. Ribes, J. Non-Cryst. Solids **57,** 49 (1983).

[10] S. R. Ovshinsky, in: Insulating and Semiconducting Glasses, Series on Directions in Condensed Matter Physics, vol. 17, (ed. P. Boolchand), World Scientific, London, 2000, p. 729; T. Ohta, J. Optoelectr. and Adv. Materials **3**, 609(2001).
[11] T. Wagner, M. Frumar, S. O. Kasap, Mir. Vlcek and Mil. Vlcek, J. Optoelectr. and Adv. Materials 3 (2001) 227.
[12] T. Wagner, V. Perina, M. Vlcek, M. Frumar, E. Rauhala, J. Saarilahti, P. J. S. Ewen, J. Non-Cryst. Solids **212,** 157 (1997).
[13] T. Wagner, et. al., Solid State Ionics **141-142**, 387 (2001).
[14] J. Saarilahti, E . Rauhala, Nucl. Instrum. Methods B **64,** 734 (1992).
[15] T. I. Kosa, T. Wagner, P.J. S. Ewen, A. E. Owen, Phil. Mag. B **71,** 311 (1995).
[16] R. Swanepoel, J. Phys. E.: Sci. Instrum. **16,** 1214(1983).
[17] A. V. Kolobov, S. R. Elliott, Advances in Physics **40**, 625 (1991).
[18] T. Wagner, M. Vlcek, V. Smrcka, P. J. S. Ewen, A. E. Owen, J. Non-Cryst. Solids **164-166**, 1255 (1993).
[19] Y. Miyamoto, M. Itoh, Ke. Tanaka, Sol. State Commun. **92**, 895 (1994).
[20] T. Wagner, S. O. Kasap, M. Vlcek, A. Sklenar, A. Stronski, J. Mat. Sci. **33**, 5581 (1998).
[21] A. P. Firth, A. E. Owen, P.J. S. Ewen, in: The Structure of Non-Crystalline Materials, Taylor and Francis, London, p. 231, 1983.
[22] G. Lukovski, F. L. Geils, R. C. Keezer, The Structure of Non-Crystalline Materials, Taylor and Francis, London, p. 127, 1977.
[23] G. Lukovski, R. M. Martin, J. Non-Cryst. Solids **8-10**, 185 (1972).
[24] T. Mori, S. Onari, T. Arai, Jap. J. Appl. Phys. **19**, 1027 (1980).
[25] P. Nagels, E. Sleeckx, R. Callaerts, L. Tichy, Solid State Commun. **94**, 49 (1995).
[27] A. Sklenar, M. Vlcek, P. Bezdicka, Proceedings of the 5th ESG Conference ìGlass Science and Technology For 21st Century, (Helebrant A., Maryska M., Kasa S., eds.), Czech Glass Society, Praha, p.C1-99, 1999.
[28] G. Lucovski, F. L. Galeener, R. C. Keezer, R. H. Geils and H. A. Six, Phys. Rev. B **10**, 5134 (1974).
[29] K. Jackson, A. Briley, S. Grossman, D. V. Porezag, M. R. Pederson, Phys. Rev. B **60**, R14985 (1999).
[30] H. Takebe, H. Maeda, K. Morinaga, J. Non-Cryst. Solids **291**, 14 (2001).
[31] H. Schmalzried, Solid State Reactions, Academic Press, New York, 1974.
[32] A. Feltz, Amorphous Inorganic Materials and Glasses, VCH Weinheim, 1993.